ARID ZONE JOURNAL OF ENGINEERING, TECHNOLOGY & ENVIRONMENT
AZOJETE December 2024. Vol.20(4):828-835
Published by the Faculty of Engineering, University of Maiduguri, Maiduguri, Nigeria.
Print ISSN: 1596-2490, Electronic ISSN: 2545-5818
www.azojete.com.ng

ORIGINAL RESEARCH ARTICLE

SOLIDWORKS MODELING OF MECHANICAL STRENGTH OF AN OPTIMUM HIGH PRESSURE A360 DIE CAST

N. O. Ubani[1*], J. E. Dara[2] and V. C. Ezechukwu[3]

[1]*Department of Mechanical Engineering, Michael Okpara University of Agriculture, Nigeria*
[2]*Department of Mechanical Engineering, Nnamdi Azikiwe University, Awka; Nigeria*
[3]*Department of Mechanical Engineering, Chukwuemeka Odumegwu Ojukwu University, Uli, Nigeria.*
**Corresponding author's email address: grantnelson2015@gmail.com*

ARTICLE INFORMATION

Submitted 04 June, 2024
Revised 29 July, 2024
Accepted 08 Aug., 2024

Keywords:
Discretization
Mesh, nodes
Tensile load
Flexural load

ABSTRACT

In this study, SolidWorks modeling was utilized to analyze the mechanical strength of high pressure A360 die castings. The model incorporates all necessary factors, such as material properties and design features, to accurately predict the tensile strength and flexural strength of A360 die cast components. From the input data, a statistical analysis was performed to identify key factors that affect the mechanical strength of the die cast materials. These factors were then used to build a regression model that accurately predicts the mechanical strength of the materials. By simulating various stress and strain scenarios, this research provides an in-depth understanding of the material's strength and its behavior under different loading conditions. The results showed that the maximum tensile stress of 13.401 MPa was recorded on application of 1000 N tensile load. The maximum elongation associated with 1000 N tensile load was 0.0139 mm. The maximum stresses due to concentrated and distributed 1000 N flexural loads were 66.820 MPa and 43.506 MPa respectively. The maximum deflection of 0.0527 mm was recorded due to concentrated flexural load of 1000 N and the maximum deflection due to distributed flexural loading of 1000 N/mm was 0.0371 mm. The results of this study can be used to optimize the design process of high pressure A360 die cast components, leading to improved performance and increased reliability. This will greatly aid in the design and manufacturing process, allowing for optimized designs and improved product performance. This study serves as a valuable resource for engineers and manufacturers looking to optimize the mechanical strength of their high pressure A360 die castings.

1.0 Introduction

Aluminum and its alloys can be melted down and be reused over and over again without any detriment to its mechanical properties. Aluminum and its alloys are the most popular metal used in engineering applications besides iron and steel. They are widely used in transportation, defense, construction, aerospace, maritime, domestic, and general engineering purpose (Mohiuddin *et al.,* 2015). The requirement of aluminum alloy part is unavoidable in transportation sector due to their light weight leading to energy savings and less emissions and mass production of aluminum alloys is supported high pressure die cast process (Rathinam *et al.,* 2021). Thirugnanam (2013) reported that about 70% of aluminum castings are produced using high-pressure die casting process.

Aluminum products are made in a variety of ways that aim to improving the mechanical properties of the finished products or to achieving a desired property within a specific range, some of the common methods of manufacturing aluminum products include extrusion, forging, drawing, rolling, and casting. Pure aluminum is soft having comparatively poor casting features and little strength, that's why aluminum castings are prepared from aluminum alloys (Mohiuddin *et al.,* 2015). Aluminum alloys are widely used in die casting process because

of their good combination of strength and light weight (Hu *et al*., 2006). High pressure die casting is an economical fusion technique that can produce several complex shapes (Mohamad et al., 2020). Due to the external high pressure, it is possible to flow the molten metal into every corner of the complex shape of a cavity hence the complex shape of the casting can be easily produced (Tariq *et al.,* 2022). Aluminum alloy castings are extensively used in general engineering, automobile, aerospace industries due to their excellent cast-ability, machinability, corrosion resistance and high strength-to-weight ratio (Mohiuddin *et al.,* 2015). When the optimal processing technology parameters are applied, the castings with very less porosities can be obtained (Amitkumar et al., 2015; Mohammad, 2015; Balikai *et al.,* 2018; Rathinam *et al*., 2021; Tariq *et al.*, 2022). Ubani (2023) reported the optimal process parameters for high pressure die casting of A360 as 1st stage plunger velocity of 0.15 m/s, 2nd stage plunger velocity of 3.0 m/s, intensification pressure of 25 MPa, pouring temperature of 680°C, and shot chamber temperature of 100°C. These optimal process parameters were used to produce the optimum high pressure A360 die cast. The aim of this work is to use SolidWorks modeling to investigate the tensile strength and the flexural strength of the optimum high pressure A360 die cast.

2. Materials and Methods

2.1 Materials

The materials that were used for the study are aluminum coil sourced from Cutix PLC Nnewi, Anambra State. Silicon, magnesium, iron, manganese, nickel, zinc, and copper bought from Sunlabi Global International (Ltd) Jos, Plateau State.

2.2 Method

The samples of A360 (ANSI/AA A360.0) alloy were produced via high pressure die casting process. The produced samples have compositions of the alloying metal as follow: 10wt% silicon, 0.6wt% magnesium, 1.3wt% iron, 0.35wt% manganese, 0.5wt% nickel, 0.5wt% zinc, and 0.6wt% copper. The process parameters of the high pressure die casting machine were set manually via the programmable logic control panel board with 1st stage plunger velocity of 0.15 m/s, 2nd stage plunger velocity of 3.0 m/s, intensification pressure of 25 MPa (Ubani, 2023). The aluminum alloy was heated to 700°C and the temperature was held at 680°C before ladled into the die casting machine from the holding furnace with the help of the tong. The shot chamber of the die casting machine was initially preheated to a temperature of 100°C. The casting process is as follows: clamping of die, injection of molten metal, cooling of molten metal, ejection of cast, and trimming of cast (Mohamad *et al.,* 2020). The samples were prepared according to ASTM standard. The dumbbell shaped samples were made using Taylor Hobson pantograph engraving machine equipped with milling attachment. Tensile testing of the samples was conducted on the A360 cast in accordance with the ASTM E8 (2024) standard on round tension test specimens of gauge length 25mm using Ametek Ez-250 digital tensile and compression tester. It was conducted at room temperature. The ultimate tensile strength, percentage elongation, and quality index of the specimens were also determined. The cross-sectional areas were measured using Mitutoyo digital vernier caliper of precision 0.01mm, while the gauge lengths of 50mm were marked on the samples. Each sample was mounted on the tensile clamps. The extensometer was zeroed and travel speed of 2mm per minute was selected (Goanta, 2020). Peak force and extension were displayed at the end of the test. Raw data of applied forces with the corresponding increases in length were saved in the computer. The stress-strain curves, ultimate tensile strength, yield strength and yield point, Young's modulus, tensile toughness and percentage of elongation were subsequently derived. These material properties were used to create the samples subjected to SolidWorks modeling. The SolidWorks modeling of the A360 was carried out by creating the model of the sample in the graphics area. The model was selected and mashed to give 6985 elements with 1194 nodes. The meshed model was restrained before applying tensile and flexural loads. The analysis of the model was conducted to produce the deformation and stress results. The mesh information and material properties of A360 used in the tensile and flexural testing is presented in Table 1. Figure 1 showed the mesh model of the sample used in the SolidWorks modeling and analysis of the optimal cast sample. The sample was discretized into 6985 elements with 11194 nodes.

Corresponding author's email address: grantnelson2015@gmail.com

Table 1: Mesh information and material properties

Total Nodes	11194
Total Elements	6985
Maximum Aspect Ratio	3.2582
% of elements with aspect ratio <3	99.9
% of elements with aspect ratio > 10	0
% of distorted elements (Jacobian)	0
Material Name	A360 Cast
Model type	Linear Elastic Isotropic
Default failure criterion	Maximum von Mises Stress
Yield strength	5.51485e+007N/m^2
Tensile strength	1.24084e+008N/m^2
Elasticmodulus	6.9e+010 N/m^2
Poisson's ratio	0.33

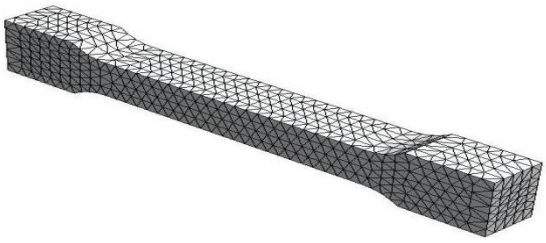

Figure 1: Solid mesh of the sample

The left-hand side of the sample was fixed, and a tensile force was applied on opposite side. Von Mises failure criterion was used to evaluate the potential safe application of the cast.

3. Results and Discussion

The samples produced using these optimal process parameters of 1st stage plunger velocity of 0.15 m/s, 2nd stage plunger velocity of 3.0 m/s, intensification pressure of 25 MPa, pouring temperature of 680°C, and shot chamber temperature of 100°C were subjected to tensile loading forces of 200 N, 600N, and 1000N and the results were presented in Figures 2 – 19.

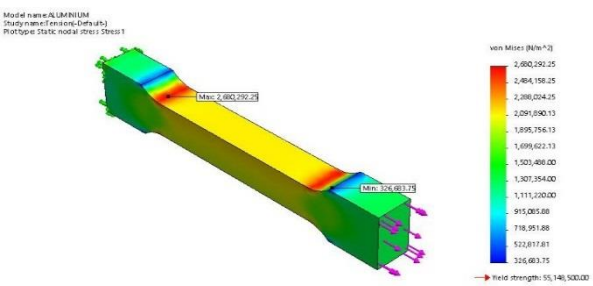

Figure 2: Tensile stress due to 200 N load

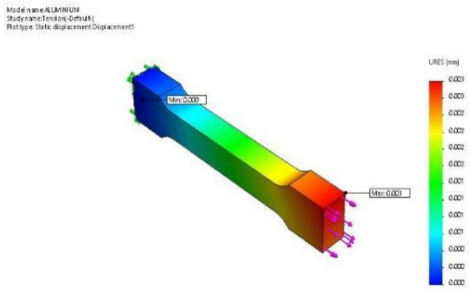

Figure 3: Tensile displacement due to 200 N load

Figure 2 depicted the tensile stress induced in the sample due to a tensile force of 200 N. The maximum stress is 2.68 MPa and the minimum stress is 0.327 MPa, but the yield strength of the material is 55.15 MPa. The maximum stress occurred at the center of the arc of curvature of the chamfered portion of the sample due to stress concentrations. The maximum stress occurred at node 11087 while the minimum stress occurred

Corresponding author's email address: grantnelson2015@gmail.com

at node 8760. Since the maximum induced stress is very low compared to the yield strength of 55.15 MPa, it implies that the material will not fail due to application of static tensile load of 200 N (Ubani *et al*., 2023). The tensile elongation of the sample as a result of 200 N force is represented in Figure 3. The maximum extension of 0.003 mm occurred at the point of application of the force whereas no extension occurred at fixed point. In other words, there is no extension at the fixed point. The maximum elongation of 0.003 mm is very insignificant. The maximum extension occurred at node 353 while the minimum extension occurred at node 31.

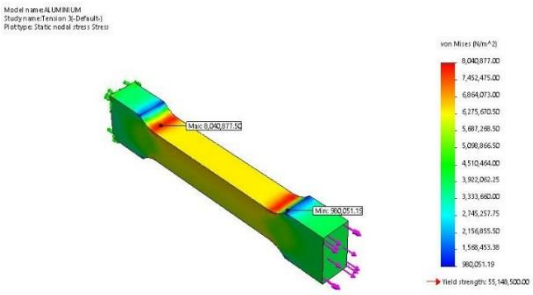

Figure 4: Tensile stress due to 600 N load

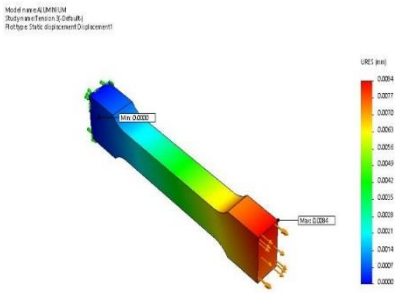

Figure 5: Tensile displacement due to 600 N load

The tensile stress of the sample subjected to tensile force of 600 N is shown in Figure 4. The maximum stress of 8.04 MPa occurred at node 11087 while the minimum stress of 0.890 MPa occurred at node 8760. The maximum stress is less than the yield strength of the material which is 55.15 MPa. Correspondingly, the maximum induced stress is very low compared to the yield strength, it indicates that the material will not fail at application of static tensile load of 600 N. Figure 5 presented the tensile elongation of the sample as a result of 600 N force. The maximum extension of 0.0084 mm occurred at the point of application of the force while the fixed point remained unaltered with no extension. The maximum extension occurred at node 353 while the minimum extension occurred at node 31 (Goanta, 2020). The maximum extension of 0.0084 mm is negligible.

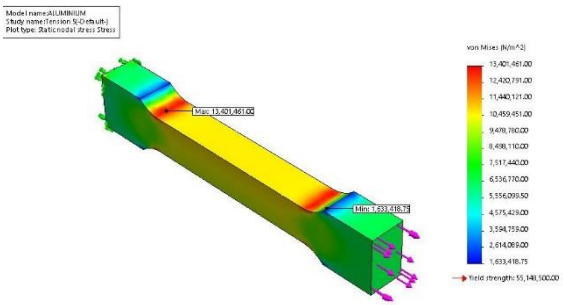

Figure 6: Tensile stress due to 1000 N

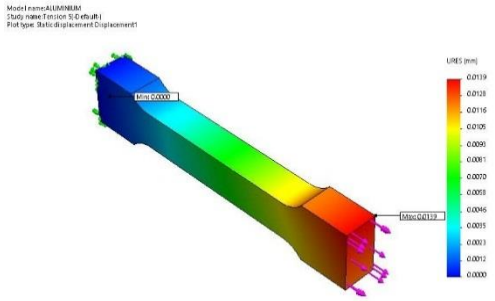

Figure 7: Tensile displacement due to 1000 N

Corresponding author's email address: grantnelson2015@gmail.com

Figure 6 illustrated the sample subjected to tensile stress due to tensile force of 1000 N. The maximum stress of 13.401 MPa occurred at node 11087 while the minimum stress of 1.633 MPa occurred at node 8760. Comparing the maximum stress with the yield stress of the material which is 55.15 MPa gave a factor of safety of 4.115. It implies that the material can withstand the applied load of 1000 N without failure. Figure 7 depicted the tensile elongation of the sample as a result of application of 1000 N force. The maximum extension of 0.0139 mm occurred at the point of application of the load while the fixed point remained intact with no extension. The maximum extension occurred at node 353 while the fixed point corresponds to node 31. The maximum extension of 0.0139 mm is slightly significant. It could be observed that for all the different amounts of loading, the maximum stress occurred at node 11087 and the minimum stress occurred at node 8760. Node 11087 is at the center of the arc of curvature that formed the chamfered portion of the sample. There is stress concentration in this portion of the sample due to change in the geometry of the sample. Despite the stress concentration in the sample, the maximum stress developed in the sample is considerable below the yield strength of the A360 cast. Also, the cast A360 is not very ductile since the elongation during loading is very minimal. Thus, the cast A360 can safely sustain a static loading up to 1000 N without failure (Ubani *et al.*, 2023).

One major possible application of the developed A360 cast is motorcycle clutch handle which is subjected to flexural loading during operation. Thus, the optimal cast samples of A360 were subjected to both concentrated and distributed flexural loadings of 200 N to 1000 N. The ends of the sample were fixed during the testing while gauge lengths were subjected to loading. The maximum deflection of the samples occurred at the center of the test samples.

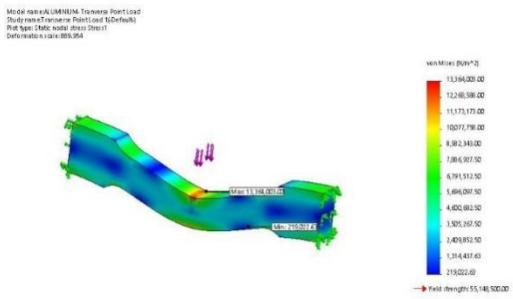

Figure 8: Flexural stress due to 200 N load

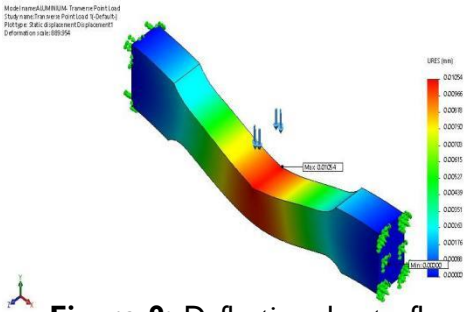

Figure 9: Deflection due to flexural load of 200 N

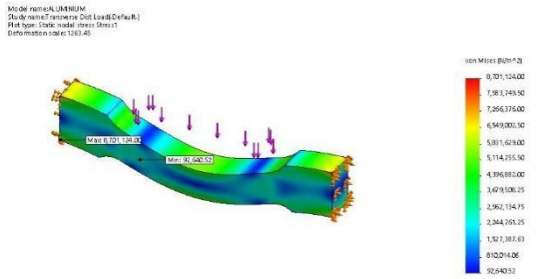

Figure 10: Flexural stress due to 200 N/mm

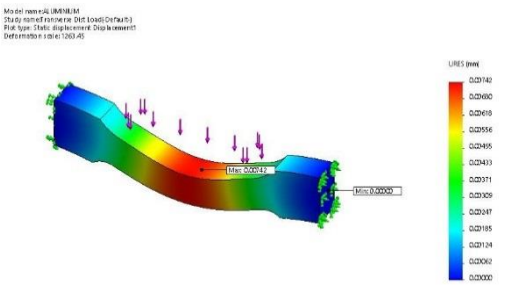

Figure 11: Deflection due to flexural loading of 200 N/mm

Corresponding author's email address: grantnelson2015@gmail.com

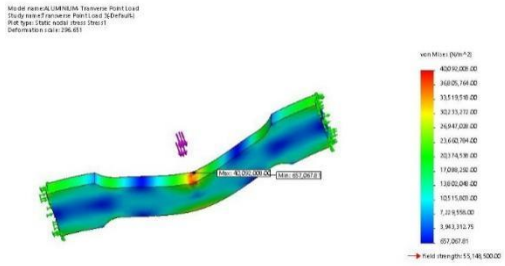

Figure 12: Flexural stress due to 600 N load

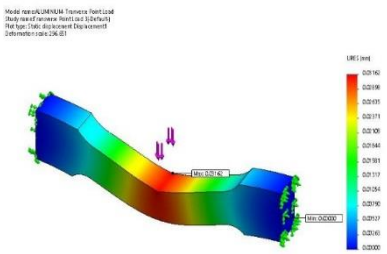

Figure 13: Deflection due to flexural load of 600 N

Figure 8 depicted the flexural stress due to a concentrated load of 200 N. The maximum stress of 13.364 MPa occurred at node 11307 which coincides with the center of the sample. The minimum stress of 0.219 MPa occurred at node 8709. The maximum deflection of 0.01054 mm as a result of 200 N loading occurred at node 11306 as shown in Figure 9. The deflection was magnified to the scale of 889.95. The fixed points did not deflect as expected. Figure 10 presented the stress owing to the distributed loading of 200 N/mm. The maximum stress is 8.701 MPa and the minimum stress is 0.093 MPa. The maximum stress occurred at node 74 while the minimum stress occurred at node 9677. It could be seen that the concentrated load exerts more stress on the sample and their maximum values do not occur at the same node for loading of 200 N. In both cases, the maximum stress is less than the yield stress of 55.15 MPa. As depicted in Figure 11, the maximum deflection due to distributed loading of 200 N/mm is 0.0074 mm and it occurred at node 6601. The deflection was magnified to the scale of 1263.45. The maximum deflections in concentrated loading and distributed loading occurred at the center of the samples while their fixed points did not deflect. The concentrated load of 200 N produced a larger deflection than the distributed load. The defections recorded for both cases are very negligible.

Figures 12 and 14 depicted the flexural stress due to a concentrated and distributed loading of 600 N and 600 N/mm respectively. The concentrated loading exerted a maximum stress of 40.092 MPa at node 11307 while the distributed loading exerted a maximum stress of 26.103 MPa at node 74. The minimum stress due to the point load is 0.647 MPa and occurred at node 8709, while the minimum stress due to the distributed load is 0.277 MPa and occurred at node 9677. Similarly, the concentrated load exerts more stress on the sample than the distributed loading and their maximum values do not occur at the same node. In both cases, the maximum stress is less than the yield stress of 55.15 MPa, which implies that the cast A360 can withstand both concentrated and distributed load of 600 N and 600 N/mm. The produced A360 cast can support moderate concentrated and distributed flexural loads (Ubani *et al.,* 2023). Figure 13 depicted the deflection due to 600 N concentrated load. The maximum deflection of 0.0316 occurred at node 11306. The deflection was magnified to the scale of 296. Figure 15 showed the deflection due to distributed loading of 600 N/mm. The maximum deflection of 0.0223 mm occurred at node 6601 with deflection was magnified to the scale of 421. The maximum deflections in concentrated and distributed loadings occurred at the center of the samples while their fixed points did not deflect. The values of the defections recorded in both cases are insignificant.

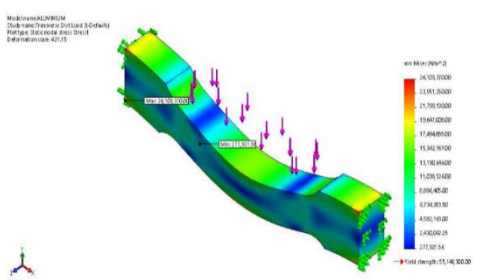

Figure 14: Flexural stress due to 600 N/mm

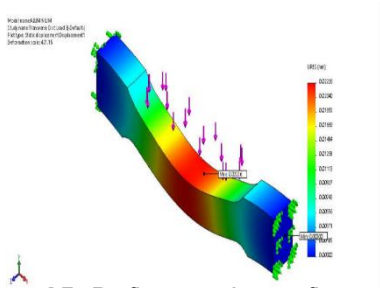

Figure 15: Deflection due to flexural loading of 600 N/mm

Corresponding author's email address: grantnelson2015@gmail.com

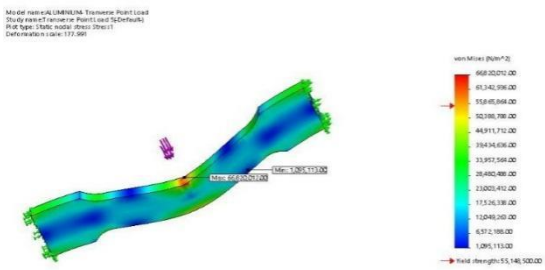

Figure 16: Flexural stress due to 1000 N load

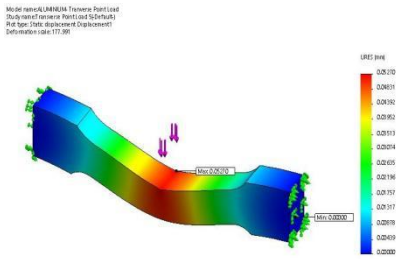

Figure 17: Deflection due to flexural load of 1000 N

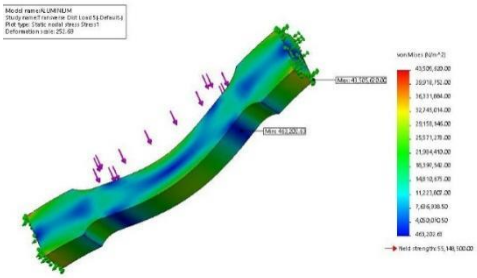

Figure 18: Flexural stress due to 1000 N/mm

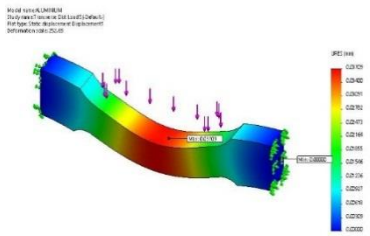

Figure 19: Deflection due to flexural loading of 1000 N/mm

Figure 16 depicted the flexural stress due to a concentrated load of 1000 N, whereas Figure 18 represented the stress owing to the distributed loading of 1000 N/mm. The maximum stresses due to concentrated and distributed loads are 66.820 MPa occurring at node 11307 and 43.506 MPa occurring at node 74 respectively. The minimum stress owing to concentrated load is 1.095 MPa occurring at node 8709 and the minimum stress owing to distributed load is 0.463 MPa occurring at node 9677. The maximum stress (66.820 MPa) induced by the concentrated load of 1000 N is higher than the yield stress of 55.15 MPa. Therefore, the developed A360 cast is very likely to failure by the application of static concentrated load of 1000 N; though, it might not fail by application if static distributed load of 1000 N/mm. The maximum deflection of 0.0527 mm was recorded due to concentrated load of 1000 N occurring at node 11306 as shown in Figure 17. The deflection was magnified to the scale of 177.99. As shown in Figure 19, the maximum deflection due to distributed loading of 1000 N/mm is 0.0371 mm and occurred at node 6601. The deflection was magnified to the scale of 252.69. The maximum deflections in concentrated loading and distributed loading occurred at the center of the samples while their fixed points did not deflect. The defections recorded for both cases are insignificant. It could be observed that as both concentrated and distributed loadings increase, the stresses and deformations increase as well. Even though the values of responses varied with amount of loading, all occurred at the same points. The maximum stress and deflection occurred at the center of the samples. The developed A360 cast can withstand distributed static loads up to 1000 N/mm without failure. It can withstand concentrated static loads up to 800 N; but it cannot safely support a concentrated load of 1000 N. The maximum flexural strength, ultimate tensile strength and percentage elongation for A360 cast recorded via experiment were 142.85 MPa, 83.442 MPa and 19.78 % respectively (Ubani *et al.,* 2023).

4. Conclusion

SolidWorks modeling has been employed to investigate the tensile strength and the flexural strength of the optimum high pressure A360 die cast. It was observed that the developed A360 cast can safely sustain a static tensile load up to 1000 N without failure. It can withstand distributed static flexural loads up to 1000 N/mm without failure. Moreover, it can withstand concentrated flexural static loads up to 800 N; but it cannot safely support a concentrated flexural load of 1000 N. The developed material has very low ductility since the maximum elongation induced by static tensile load of 1000 N is 0.0139 mm. Also, the defections recorded owing to concentrated and distributed flexural loads are insignificant. The developed A360 cast can be employed in the manufacturing of motorcycle clutch handle.

Corresponding author's email address: grantnelson2015@gmail.com

References

Amitkumar, A., Arunkumar, Y. and Srinath, MS. 2015. Simulation of high pressure die casting process for identifying and minimising defects. International Journal of Engineering Research & Technology (IJERT), 3(17): 1-9.

ASTM International 2024. Standard Test Methods for Tension Testing of Metallic Materials. ASTM International, 100 Barr Harbor Drive, West Conshohocken, PA 19428-2959. United States.

Balikai, VG., Siddlingeshwar, IG. and Gorwar, M. 2018. Optimization of process parameters of high pressure die casting process for ADC12 Aluminium alloy using Taguchi method. International Journal of Pure and Applied Mathematics, 120(6): 959-969.

Goanta, V. 2020. Extensometer for Determining Strains on a Tensile and Torsion Simultaneous Load. Sensors, 20(2): 385.

Hu, B., Xiong, S., Masayuki, M., Yoshihide, M. and Shingo, I. 2006. Study on vacuum die casting process of aluminum alloys. World Foundry Congress, WFC 06, 179: 1-9.

Mohamad, EM., Tommaso, M., Pasquale, B., Leonardo, G., Enrico, S. and Archimede, F. 2020. Design optimization of gate system on high pressure die casting of AlSi13Fe alloy by means of finite element simulations. Procedia CIRP, 88: 509–514.

Mohammad, S. 2015. Optimization product parts in high pressure die casting process. Materials Science and Technology, Mälardalen University Press Licentiate, Västerås Theses No. 197.

Mohiuddin, MV., Krishnaiah, A. and Hussainy SF. 2015. Influence of sand molding process parameters on product quality of Al-Si alloy casting - an ANOVA approach. International Journal of Advance Research in Science and Engineering, 4(01): 1751.

Rathinam, N., Dhinakaran, R. and Sharath, E. 2021. Optimizing process parameters to reduce blowholes in high pressure die casting using Taguchi methodology. Materials Today: Proceedings, 38, Part 5: 2871-2877.

Tariq, S., Tariq, A., Masud, M., and Rehman, Z. 2022. Minimizing the casting defects in high-pressure die casting using Taguchi analysis. Scientia Iranica B, 29(1): 53-69.

Thirugnanam, M. 2013. Modern High Pressure Die-casting Processes for Aluminum Castings. Transactions of 61st Indian Foundry Congress, January 27-29, Kolkata, 1-7.

Ubani, NO. 2023. Empirical model for predicting the defects and mechanical properties of die cast aluminum product, PhD Thesis submitted to Department of Mechanical Engineering, Chukwuemeka Odumegwu Ojukwu University, Uli.

Ubani, NO., Nwobi-Okoye, CC., Dara, JE., Eni-Ikeh, SN. and Okoro, C. 2023. Optimizaion approach for evaluation of mechanical properties of high pressure die cast aluminum alloyed product. Umudike Journal of Engineering and Technology (UJET), 9(1): 46 – 54.

Corresponding author's email address: grantnelson2015@gmail.com